International Journal of Precision Engineering and Manufacturing Vol.6, No.2, April 2005.

Numerical and Experimental Investigation on the Tube Forming in the Radial-Forward Extrusion

Beong-Du Ko[1], Dong-Hwan Jang[1], Ho-Joon Choi[1] and Beong-Bok Hwang[2,#]

[1] Department of Automation Engineering, Inha University, Inchon, South Korea
[2] Department of Mechanical Engineering, Inha University, Inchon, South Korea

ABSTRACT

In this paper, the tube forming by radial-forward extrusion is analyzed by numerical simulation and experiments. The paper discusses the effect of process variables such as gap height, relative gap width and die corner radius on tube forming. The influence of deformation patterns of flange in radial extrusion on forward extrusion for tube forming is investigated and summarized in terms of the maximum forming force and hardness variations along the extrusion path. Furthermore the external defects are shown experimentally during the forming operation. Based on finite element analysis in conjunction with experimental test in Al alloy, analysis is performed for important parameter combination in order to reduce forming defects. Eventually, the process parameters for safe forming are suggested in order to reduce the forming defects.

Key Words : Combined extrusion, Radial-forward extrusion, Tube forming, Tool geometry, Forming defect

1. Introduction

There are four basic types of extrusion: direct (forward) and indirect (backward), hydrostatic, and impact. In direct extrusion, the part is extruded in the direction of punch movement[1], while the product is extruded in the direction opposite to that of punch travel in indirect extrusion. In hydrostatic extrusion, the chamber is filled with fluid that transmits the pressure to the billet, which is then extruded through the die. Impact extrusion is a form of indirect extrusion and is particularly suitable for hollow shapes[2].

In addition to these four basic types, radial extrusion is used to produce parts that generally feature a central hub with radial protrusions[3,4]. As opposed to conventional forward and backward extrusions, in which the material flows in a direction parallel to that of the punch or die motion, in radial extrusion the material flows perpendicular to the punch motion. The deformation of complex parts such as universal joints, tube fittings, and differential gears usually involves some form of radial extrusion, combined with other processes such as upsetting and/or forward and backward extrusion[5,6].

Generally, the tube forming is performed by hydro-forming, drawing, welding chamber type extrusion, incremental forming process such as swaging, and extrusion with the use of a mandrel. However, the tube forming by the radial extrusion combined with subsequent forward can extrusion is possible with one outlet orifice where the partial processes are executed one after the other, i.e. forward after radial.

In this study, the process sequence to combine radial extrusion with subsequent forward can extrusion is applied to analyze the forming characteristics. Selected design parameters include the gap height that is determined by the gap between container and mandrel, and the relative gap width that is defined by a

Manuscript received: February 6, 2003;
Accepted: August 4, 2004
Corresponding Author:
Email: bbhwang@inha.ac.kr
Tel: +82-32-860-7387, Fax: +82-32-860-7387

relationship between the gap height and the annular gap in which material flows to form a tube shape. Both numerical and experimental studies have been conducted to observe the possible failures during the process particularly in experiments. A rigid-plastic finite element method is also applied to the forming process to compare the deformation pattern with the experiments and to see the material flow during the process in detail.

2. FEM Analysis and Experiments

2.1 Stress-Strain Relationship

Usually in hot forging operation, the flow stress is influenced significantly by the strain rate, but in cold forging the flow stress depends mainly on the strain itself. The flow stress-strain relationship can be approximated by[7]:

$$\bar{\sigma} = K\bar{\varepsilon}^{n} \tag{1}$$

where K is known as the strength coefficient and n the strain hardening exponent. Generally, there are two ways to obtain the values of K and n : an experimental method[8] and an analytical method[9]. In this paper, the material properties, the strength coefficient K and the strain hardening exponent n, were determined through a uniaxial compression experiment. In this study, the material used for the experiment and the simulation is commercially available AA 3105 aluminum alloy. The experiment to obtain the material properties was performed under room temperature and the relationship between flow stress and effective strain for AA 3105 could be approximated by

$$\bar{\sigma} = 280.3\bar{\varepsilon}^{0.17} \quad (MPa) \tag{2}$$

2.2 Ring Compression

In analyzing the mechanics of metal-forming processes, a realistic friction condition must be specified in order for a theory to yield a reliable solution. Also, in practice, understanding and controlling friction often leads to successful metal forming operations. Consequently, considerable effort has been devoted to determining satisfactorily the friction condition in various metal forming processes[10]. Yet, the mechanism of friction is still not well known and, as Thomsen[11] has stated, friction remains one of the most elusive variables in metal forming technology.

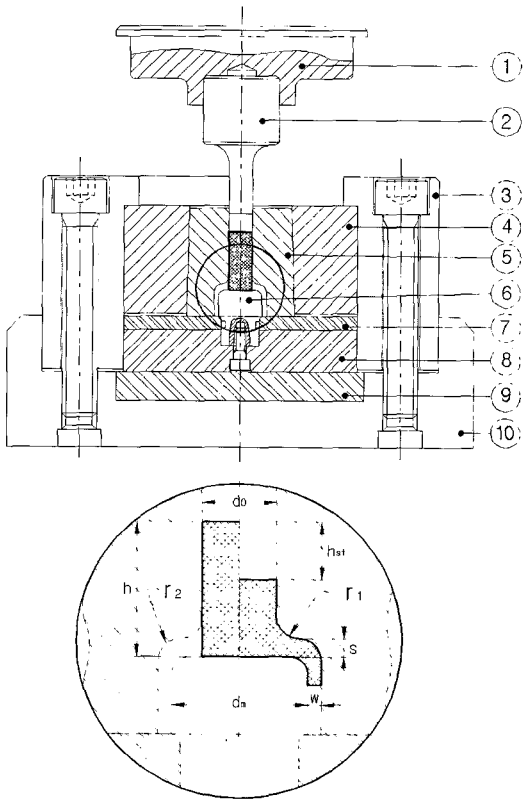

Fig. 1 Schematic illustration of the details of the tool used in the metal experiment

Table 1 Tool materials

No	Part name	Material
1	Punch holder	SM45C
2	Punch	STD11
3	Die holder	SM45C
4	Pre-stressed ring	STD11
5	Die insert	STD11
6	Mandrel	STD11
7	Spacer	SM45C
8	Lower die	STD11
9	Pressure plate	STC3
10	Die holder	SM45C

In this study, a ring compression test has been performed to obtain the value of a friction factor, m. In ring compression, friction values are evaluated by comparing the experimental data with the so-called calibration curves. However, this procedure raises some questions regarding the accuracy and efficiency of this evaluation scheme since the calibration curves are not unique and depend not only on the strain, strain-rate, and the thermal characteristics of the material, but also on the specimen geometry. Furthermore, experimental data usually do not follow the trend of the predicted curve for a constant friction value. However, the method by Hwang and Kobayashi[12] uses the finite-element technique, and includes fitting curves to the experimental data with an iteration scheme for evaluating the current friction value based on measured changes of the ring dimensions. This scheme for evaluating friction was applied to the experimental data for AA 3105 aluminum alloy, for a ring geometry of 6:3:2(outer diameter: inner diameter: thickness). Several experiments were conducted with a mixture of commercially available grease and MoS_2 as lubricant. The results led to the approximation for the friction factor to be about 0.1 with the applied lubricant.

Table 2 Parameters used in experiment and simulation

Parameters		Values
Material conditions	Material	AA 3105
	Billet size ($d_0 \times h$)	Ø16 × 45 (mm × mm)
Friction factor (m)		0.1
Geometric condition	Gap height (s)	2, 4, 6 (mm)
	Die corner radius ($r = r_1 = r_2$)	3, 5 (mm)
	Mandrel radius	2 (mm)
	Mandrel dia. (d_m)	26, 28, 30 (mm)
	Gap width (w)	2, 3, 4, 5, 6, 7.5 (mm)

2.3 Simulations and Experiments

The material properties and frictional condition from experiments such as strength coefficient, strain hardening exponent, and friction factor are applied to the finite element analysis code ALPID (analysis of large plastic incremental deformation)[13] which is programmed based on the theory of rigid plasticity and used for simulations of tube forming processes in the present study.

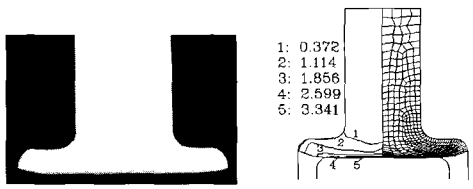

(a) Gap height(s) = 4 mm

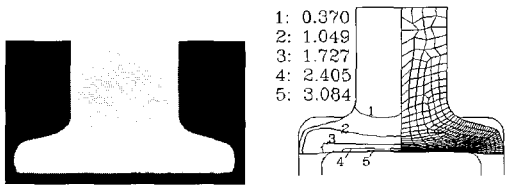

(b) Gap height(s) = 6 mm

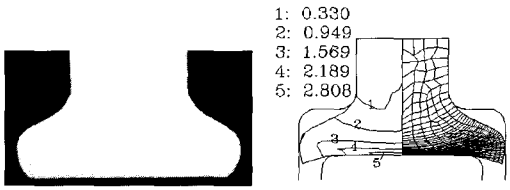

(c) Gap height(s) = 8 mm

Fig. 2 Effect of deformation patterns: Experiment (left) and simulation (right)

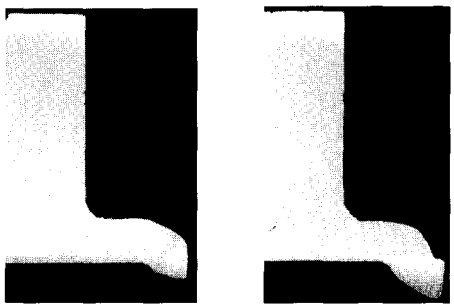

(a) w/s = 0.75 (b) w/s = 1.25

Fig. 3 Effect of relative gap width (w/s) on tube forming (stroke = 20 mm)

Experiments have been performed in a single acting hydraulic press with the frame capacity of 50 tonf. The ram speed of the press was regulated to be 1.0 mm/sec. downward for all experiments. The punch displacement was measured from the displacement indicator and encoder. A load-cell was used to pickup the value of forming load during the experiment. A die set was

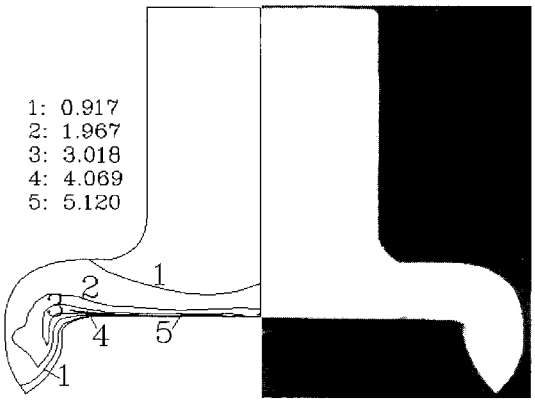

Fig. 4 Comparison of tube forming patterns between simulation (left) and experiment (right)

prepared for the experiment as shown in Fig. 1. To minimize the effect of eccentricity, the mandrel ⑩ is tightly fixed at center. The pressure ring ④ was also applied to the die set for the die insert ⑤ to maintain sufficient stiffness. Details of the die set are shown in Fig. 1 and the materials used for the die set are summarized in Table 1. Parameters used in experiments and simulations are described in Table 2. The scanning cross section of the extruded material from Fig. 2 to Fig. 5 are obtained after cut in a milling machine and polished.

3. Results and Discussion

3.1 Tube Forming Patterns

Deformation patterns from the experiments (left) and simulations (right) are shown in Fig. 2. The figure describes different flow patterns, especially at the time when the material comes to contact with the outer container. It is easily seen from the figure that the forming pattern of the flange section is very much dependent of the gap height (s), which is selected as one of major process parameters in the present study[14]. In the case of the gap height (s) of 4.0 mm, the leading edge of the flange is moving out in the radial direction separately from the mandrel surface. However, when the gap height (s) is relatively large, say 8.0 mm, the edge of flange is shown to be in contact with the mandrel throughout the radial extrusion process and the barreling phenomenon is also observed. The significant differences in the deformation patterns are shown in the figure such that the flange tip touches the outer container in different manners with different gap heights (s). In the deflection

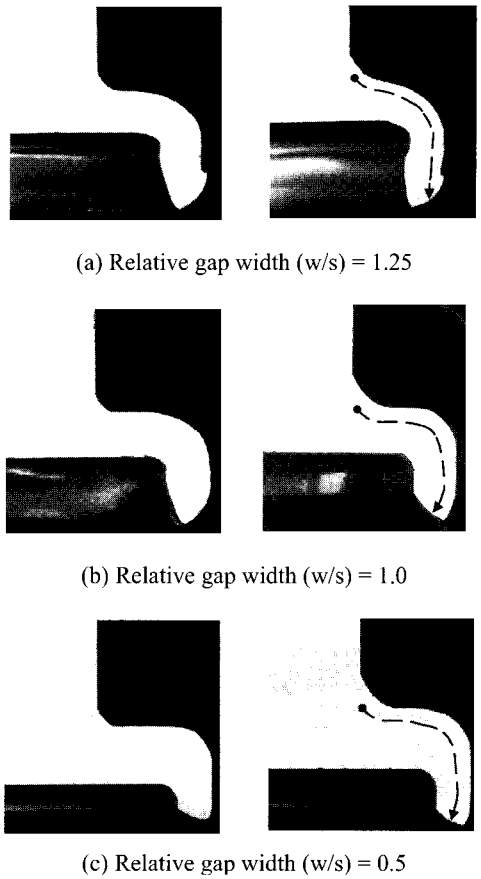

(a) Relative gap width (w/s) = 1.25

(b) Relative gap width (w/s) = 1.0

(c) Relative gap width (w/s) = 0.5

Fig. 5 The deformation patterns of tube, r = 3 (left) and r=5 (right)

area where the forward extrusion is about to start, more resistance to material flow is expected with a smaller gap height (s). It is also seen in the figure that the smaller gap height leads to the greater effective stain distribution in the workpiece.

Fig. 3 shows a comparison of deformation patterns at the time when the tube forming (forward extrusion) has just started and the punch stroke (h_{st}) reaches 20.0 mm with different relative gap widths (w/s). Note that the same gap height, i.e. 4.0 mm, is applied to both cases. As seen easily in the figure, the material is smoothly guided into the annular gap for forward extrusion when the relative gap width (w/s) is small, i.e. w/s = 0.75. The greater relative gap width set to be s/w = 1.25 leads to folding of material near the tip of flange. The forward extrusion is constrained by this folding which may help the corner filling. The figure also tells that the tube forming is very much influenced by the gap width.

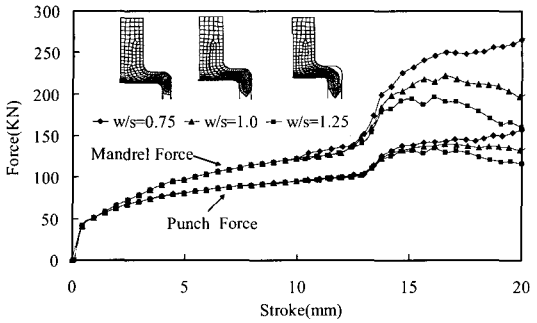

Fig. 6 Comparison of load-stroke relationship for relative gap width

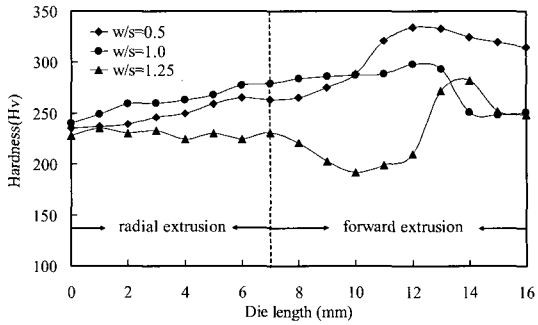

Fig. 7 Hardness variation along the extrusion path

Fig. 4 represents a comparison of tube forming patterns between the simulation and the experiment. The comparison is made for the relative gap width (w/s) of 1.0, the die corner radius (r) of 3.0 mm, and the punch stroke (h_{st}) of 23.0 mm. It is seen in the figure that the overall deformation pattern in the experiment comes out to be very similar to that in simulation. The effective strain distribution from simulation in the figure shows that the greatest effective strain appears near the contact area with the mandrel. The flow resistance is caused mainly by the contact with the mandrel. This leads to the forming of a sharp edge at the tip of the tube.

Fig. 5 shows the deformation patterns for different design parameters in experiments. Figure 5(a) shows the deformation pattern with the relative gap width (w/s) of 1.25. Regardless of the dimension of die corner radius (r), folding of material on the outer surface of the tube takes place. Folding is more significant with the die corner radius of 3.0 mm. It can be seen from the figure that the material flows more easily with the larger die corner radius (r). For the die corner radius of 5.0 mm, the material is not touching the corner of the mandrel at this moment. However, after the folding increases the flow resistance into the annular gap, the complete corner filling is obtained later in the process. The deformation pattern with the relative gap width (w/s) of 1.0 is shown in Fig. 5(b). For the die corner radius of 3.0 mm, the corner filling near the inner surface is completed while the corner near the outer surface is not filled. Furthermore, the cross section of the tip of the forward extruded material becomes thin and crack initiates at this moment. Unlike that in Fig. 5(a), the folding effect does not exist in this case and the thickness near the leading edge of the tube is formed to be thin. For r = 5.0 mm, the corner filling near the outer surface is smoothly completed. Figure 5(c) shows the deformation pattern for w/s = 0.5. In this case, the forming of a tube including corner filling is relatively in good shape comparing with those in Fig 5(a) and 5(b). It can be concluded from Fig. 5 that a large die corner radius leads to complete corner fillings both near inner and outer surfaces and thus the tube forming process is completed smoothly. Parameters influencing the radial forward extrusion process are the gap height (s) between the mandrel and die face, and the width of the annular gap (w)[3]. However, it is ascertained from the figure that the gap height (s) has greater influence on the radial extrusion process[15].

3.2 Forming Load

Usually, the forming load in the metal forming process using an open die is influenced mainly by the process condition and the material properties[16]. Figure 6 shows the load-stroke relationship from simulation for different relative gap widths (w/s) when the gap height (s) and die corner radius (r) are 4.0 mm and 3.0 mm, respectively. As shown in the figure, the forming load increases as the relative gap width (w/s) decreases. It can be confirmed from the figure that the forward extrusion is about to start when the punch stroke reaches about 13.0 mm, at which point the forming load changes abruptly. The effect of the relative gap width (w/s) on the mandrel force is shown to be much higher than that on the punch force. It is interesting to note from the figure that the forming load on both mandrel and punch decreases with the relative gap width (w/s) of 1.0 and 1.25, as the punch stroke for forward extrusion process increases. In this case, the

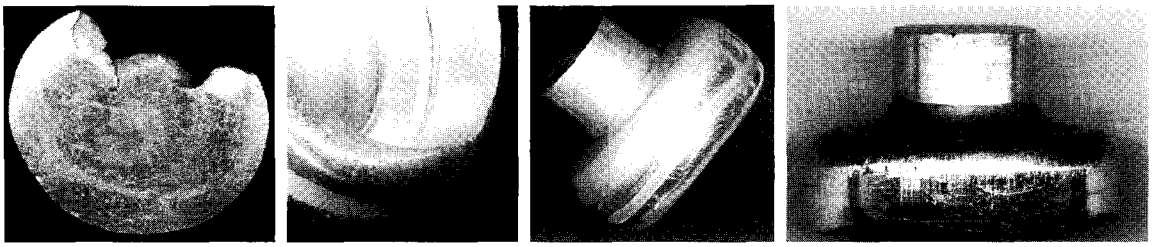

(a) Fracture (b) Crack (c) Fold (d) Defect of extruded length

Fig. 8 Defects during tube forming processes

forward extrusion is very much similar to free extrusion, which seems to lead to low mandrel forces. However, the friction force along the die-wall interface build up and the forming load increases at the same time as the forward extrusion process proceeds.

3.3 Hardness

Usually, the hardness distributions in the cold forged parts are highly related to the effective strain distributions in the parts[17,18]. As discussed earlier, the better formability of a tube and the fine size of globular grain are expected as the relative gap width (w/s) decreases. Figure 7 shows the micro-hardness distributions within the specimen for three different relative gap widths (w/s). The die corner radius (r) of 5.0 mm is applied to all experiments and a micro Vickers hardness tester is used to measure the hardness along the cross section of the extruded material at the depth of 1.0 mm from the outer surface like the hidden line in Fig. 5. It is seen from Fig. 7 that the measured hardness increases as the relative gap width (w/s) decreases. For the relative gap width (w/s) of 0.5, the hardness is measured to be lower than that for the relative gap width of 1.0 in a radial extruded part, i.e. in flange, since the deformation is not severe in that part of material. However, when it comes to the forward extrusion process, i.e. the tube forming stage, the hardness increases since the smaller gap width (w) leads to relatively severe deformation. It is also observed form the measurement that the variation of hardness is relatively large along the path of measurement for the relative gap width (w/s) of 1.25, since incomplete corner filling and folding have not led to uniform deformation comparing with others. Note that the hardness is measured to be low near the tip of the tube for all cases.

3.4 Forming Defects & Forming Limit Diagram

Fig. 8 shows various defects observed from the experiments of the tube forming process. The defects are observed mainly on the material surface and they could be classified into two categories: one is ductile fracture by severe deformation and the other the deficiency in material flow. A ductile fracture of a flange is observed during the process of radial extrusion as shown in Fig. 8 (a). Generally, ductile fractures of a flange take place near the flange tip by severe circumferential stresses[19]. This ductile fracture occurs at the punch stroke (h_{st}) of 8.0 mm for the gap height (s) of 2.0 mm. However, the direct reason why this kind of ductile fracture in this case occurs is thought to be that the severe shear deformation is concentrated at the tip of the flange when it comes to touch the outer container near the die corner. The ductile fracture has not been detected with the other cases of gap heights (s). Figure 8 (b) shows the crack on the inner surface with the relative gap width (w/s) of 1.25 and the die corner radius (r) of 5.0 mm. This crack appears on the free surface when the material is filling the corners. Folding on the outer surface of the tube is detected as shown in Fig 8 (c). These folding phenomena have been observed when the flange flows separately from the die and the value of relative gap width (w/s) is greater than 1.0. This differs from the folding that takes place by the friction on the contact surface generally in the metal forming processes[20-22]. Figure 8 (d) shows unbalanced material flow into the annular gap in tube forming. It is observed that the unbalanced material flow into the annular gap is observed when the value of relative gap width (w/s) is less than 1.0.

The forming defects observed in the experiments are summarized and a forming limit diagram is proposed in terms of relationships between the relative gap width (w/s) and the gap height (s) based on the experimental

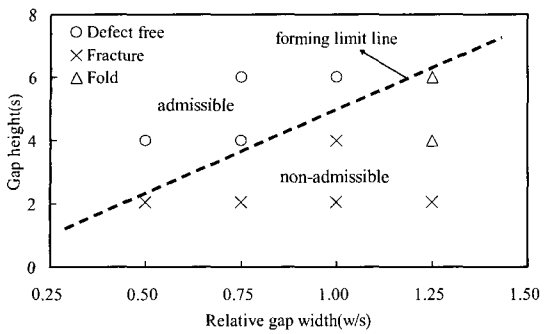

Fig. 9 Proposed forming limit diagram(r = 3 mm)

results as shown in Fig. 9. As seen in the figure, folding takes place only for the relative gap width (w/s) of 1.25 and the fracture mainly for gap height (s) of 2.0 mm. The smooth forming of a tube is expected with a large gap height (s) and with a small relative gap width (w/s).

4. Conclusions

In this paper, numerical and experimental studies have been performed to see the influence of design parameters such as the gap height, the die corner radius and the relative gap width mainly on the forming defects including formability, hardness distributions within formed parts, and the mandrel and punch loads in tube forming, i.e. radial extrusion combined with a subsequent forward extrusion process. Numerical analysis has been conducted with the use of the rigid-plastic FEM. The focus in this paper is concentrated on material failure during a tube forming process observed in the experiments. The major results can be summarized as follows:

1. The pattern of flange forming, i.e. touching the die or not, and the die corner radius affect the forming pattern of the flange tip very much.
2. The values of forming load and measured hardness are amplified with decreasing the relative gap width. The mandrel force changes more significantly than the punch force for different gap heights.
3. When the value of the relative gap width is greater than 1.0 and flange is not completely touching the die, folding phenomenon has taken place. The folding leads to secondary forming defect such as cracks on the inner surface of the tube as the process proceeds.
4. The formability of a tube enhances with increasing the gap height and with decreasing the relative gap width.
5. Forming without defects could be possible with decreasing both the gap height and the relative gap width.

References

1. Michelič, A., Štok, B., "Tool Design Optimization in Extrusion," Computers and Structures, Vol. 68, pp. 283-293, 1998.
2. Kalpakjian, S., "Manufacturing Processes for Engineering Materials," 2nd Edition, Addition-Wesley, USA, 1991.
3. Pale, J.A. and Altan, T., "Development of equipments and capabilities for investigation of the multi-action forming of complex parts," Eng. Res. Center Net Shape Manuf., p.8, 1989.
4. Lin, F. C. and Lin, S. Y., "Radius Ratio Estimation and Fold Situation Prediction of the Deformation Profile in Forging-Extrusion Process," Computers and Struc- tures, Vol. 80, pp. 1817-1826, 2002.
5. Lee, Y. S., Hwang, S. K., Chang, Y. S. and Hwang, B. B., "The Forming Characteristics of Radial-Forward Extrusion," J. of Mater. Proc. Tech., Vol. 113, pp. 136-140, 2001.
6. Choi, H. J., Choi, J. H. and Hwang, B. B., "The Forming Characteristics of Radial-Backward Extrusion," J. of Mater. Proc. Tech., Vol. 113, pp. 141-147, 2001.
7. Air Force Materials Laboratory, "Forging Equipment, Materials and Practices," Metals and Ceramics Information Center, p. 164, 1973.
8. Paul De Garmo, E., "Material and Processes in Manufacturing, Macmillan," New York, p. 27, 1967.
9. Paul De Garmo, E., "Material Properties and Manufacturing Processes," Malloy, Ann Arbor, MI, p.31, 1966.
10. Schey, J. A., Ed., "Metal Deformation Processes-Friction and Lubrication," Marcel Dekker, New York, 1970.
11. Thomson, E. G., "Friction in Forming Processes," Annuls CIRP, Vol. 17, p. 149, 1969.
12. Hwang, S. M. and Kobayashi, S., "A Note on

Evaluation of Interface Friction in Ring Test," Proc. NAMRC XI, University of Wisconsin, Madison, WI, p. 193, 1983.
13. Oh, S. I., Lahoi, G. D., Altan, T., "ALPID-a General Purpose FEM Program for Metal Forming," Proceeding of NAMRC. IX, State College, Pennsylvania, 1981.
14. Ko, B. D., Lee, S. H., Kim, D. J. and Hwang B.B., "The Influence of Die Geometry on the Radial Extrusion Processes," J. of Material Processing Tech., Vol. 113, pp. 109-114, 2001.
15. Lee, S.H., "Forming characteristics of radial extrusion, Master Dissertation," Inha University, Inchon, Korea, p. 20, 1999.
16. Walters, J., Kurtz, S., Wu, W. T. and Tang, J., "The 'State of Art'in Cold Forming Simulation," J. of Material Processing Tech., Vol. 71, pp. 64-70, 1997.
17. Rodrigues, J. M. C., Peterson, S. B., Martins, P. A. F. and Barata Marques, M. J. M., "Towards Net-shape of Tubular Components," Int. J. of Mach. Tools Manufact., Vol. 36, pp. 399-409, 1996.
18. Gouveia, B. P., Rodrigues, J. M. C. and Martins, P. A. F., "Steady-State Finite Element Analysis of Cold Forward Extrusion," J. Material Processing Tech., Vol. 73, pp. 281-288, 1961.
19. Pale, J.A. and Altan, T., Development of equipments and capabilities for investigation of the multi-action forming of complex parts, Eng. Res. Center Net Shape Manuf., p.17, 1989.
20. Balendra, R. and Qin, Y., "Identification and Classification of Flow-Dependent Defects in the Injection Forging of Solid Billets," J. of Material Processing Tech., Vol. 106, pp. 199-203, 2000.
21. Wang, Z., Lu, J. and Wang, Z. R., "Numerical and Experimental Research of the cold Upsetting-Extruding of Tube Flanges," J. of Material Processing Tech., Vol. 110, pp. 28-35, 2001.
22. Colla, D., Petersen, S. B. and Martins, P. A. F., "An Investigation into the Preforming of Tubes," Int. J. of Mach. Sci., Vol. 39, No. 5, pp. 507-520, 1997.